Robustness of nonadiabatic holonomic gates

Markus Johansson,[1,2,*] Erik Sjöqvist,[1,2,†] L. Mauritz Andersson,[3,‡] Marie Ericsson,[2,§] Björn Hessmo,[1,‖]
Kuldip Singh,[1,¶] and D. M. Tong[4,**]

[1]*Centre for Quantum Technologies, National University of Singapore, 3 Science Drive 2, 117543 Singapore, Singapore*
[2]*Department of Quantum Chemistry, Uppsala University, Box 518, Se-751 20 Uppsala, Sweden*
[3]*Department of Applied Physics, KTH Royal Institute of Technology, SE-100 44 Stockholm, Sweden*
[4]*Physics Department, Shandong University, Jinan, 250100, China*

The robustness to different sources of error of the scheme for nonadiabatic holonomic gates proposed previously
[New J. Phys. **14**, 103035 (2012)] is investigated. Open system effects as well as errors in the driving fields are
considered. It is found that the gates can be made error resilient by using sufficiently short pulses. The principal
limit of how short the pulses can be made is given by the breakdown of the quasi-monochromatic approximation.
A comparison with the resilience of adiabatic gates is carried out.

PACS number(s): 03.67.Lx, 03.65.Vf, 03.65.Yz

I. INTRODUCTION

A central challenge for the realization of practically
useful quantum computation is to find systems where the
implementation of qubits and gate operations is resilient to
perturbations due to instabilities in the setup and to open
system effects. Several approaches to realize this resilience
of quantum gates have been proposed, including the use of
decoherence-free subspaces [1], noiseless subsystems [2], and
topological quantum computation [3]. One of these approaches
is holonomic quantum computation (HQC), using adiabatic
evolution [4]. This is a general procedure to build universal
sets of gates that are robust to certain kinds of parametric
noise [5] by using non-Abelian adiabatic geometric phases.

One of the most studied implementations of adiabatic
HQC is that of Duan *et al.* [6], which utilizes an array of
trapped ions that can be manipulated by laser fields. Schemes
to implement adiabatic holonomic gates have also been
proposed in superconducting nanocircuits using Josephson
junctions [7] and in semiconductor quantum dots [8]. The
gates in Refs. [6–8] have turned out to be difficult to realize
experimentally. One reason for this is the long run time
required for the desired parametric control associated with
adiabatic evolution. The run time must be long enough to
minimize nonadiabatic corrections, but sufficiently short so
that the error rate due to open system effects and instabilities
of the setup is small.

A scheme for HQC based on nonadiabatic non-Abelian
geometric phases has been proposed in Ref. [9]. This scheme
allows for universal quantum computation using gates that can
be implemented rapidly compared to the adiabatic schemes and
therefore avoids the problems associated with a long run time.
Nonadiabatic HQC has been combined with decoherence-free

subspaces [10] and applied to coupled quantum dots as well as
molecular magnets [11]. In this paper we study some aspects of
the robustness of one-qubit gates of the proposed nonadiabatic
scheme to different kinds of errors and compare it to the
robustness of the corresponding adiabatic gates based on the
Duan *et al.* scheme.

To realize quantum computation, it is necessary to bring the
error rate per gate operation down below some threshold where
error correction can be used to make the computation reliable.
This threshold error rate has been estimated in different
settings and by different authors to be somewhere between
10^{-6} and 10^{-2} [12–16]. There are many different sources
of imperfections, and their relative importance is specific to
which system is used for the implementation of the gate. We
therefore limit our study to some general sources of error
that are typically encountered in a variety of implementations.
Specifically, we study the sensitivity to decay and dephasing
and to imperfect control of the external driving fields.

Previously it has been shown that adiabatic holonomic
quantum gates are robust to first order against small random
perturbations of the path in parameter space [5]. Further
analysis of robustness to parametric noise has been carried out
in Refs. [17–20], and robustness to environmental interaction
has been studied in Refs. [21–28]. Moreover, the adiabatic
holonomic gates are insensitive to the rate at which the
evolution is driven as long as the adiabatic approximation is
valid [5].

The outline of the paper is as follows. In Sec. II we briefly
review nonadiabatic and adiabatic HQC proposed in Refs. [9]
and [6], respectively. In Sec. III we study the resilience of one-
qubit gates to decay of the excited state, dephasing, detuning,
and incorrect parameters of the driving fields. The paper ends
with conclusions.

─────────
*cqtbemj@nus.edu.sg
†erik.sjoqvist@kvac.uu.se
‡mauritza@kth.se
§marie.ericsson@kvac.uu.se
‖phyhbg@nus.edu.sg
¶sciks@nus.edu.sg
**tdm@sdu.edu.cn

II. HOLONOMIC GATES

A. The nonadiabatic gate

The one-qubit nonadiabatic gate can be implemented in a Λ
system in the following way. A pair of zero-detuned pulses with
the same real-valued pulse envelope $\Omega(t)$ couples selectively
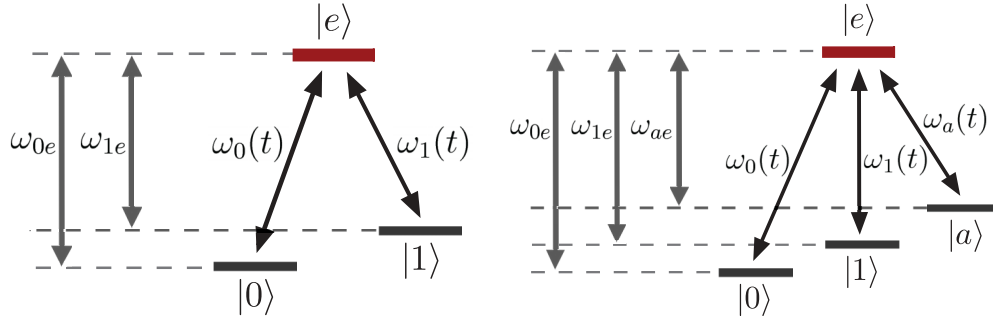two ground state levels $|0\rangle$ and $|1\rangle$ to an excited state $|e\rangle$. The

FIG. 1. (Color online) Setup for the nonadiabatic single-qubit holonomic gate in a Λ configuration (left) and for the adiabatic single-qubit holonomic gate in a tripod configuration (right). ω_{je} is the energy spacing of the $|j\rangle$ and $|e\rangle$ level, and the driving fields are $\omega_j(t) = \Omega(t)\omega_j e^{i\nu_j t}$ for $j = 0,1$ in the nonadiabatic case and $\omega_j(t) = \Omega\omega_j(t/T)e^{i\nu_j t}$ for $j = 0,1,a$ in the adiabatic case. The requirement for ideal gate implementation is $\nu_j = \omega_{je}$ in the nonadiabatic case and $\nu_0 - \omega_{0e} = \nu_1 - \omega_{1e} = \nu_a - \omega_{ae}$ in the adiabatic case. In the nonadiabatic setup the qubit is encoded in the $|0\rangle$ and $|1\rangle$ states. In the adiabtic setup the qubit is encoded in the dark subspace of the Hamiltonian. Initially the driving fields must therefore be chosen such that the dark subspace coincides with the computational subspace spanned by $|0\rangle$ and $|1\rangle$.

corresponding Hamiltonian can be expressed in the rotating wave approximation as

$$H^{(\text{na})}(t) = \Omega(t)(\omega_0|e\rangle\langle 0| + \omega_1|e\rangle\langle 1| + \text{H.c.}). \quad (1)$$

Here the complex-valued driving parameters ω_0 and ω_1 satisfy $|\omega_0|^2 + |\omega_1|^2 = 1$ and describe the relative strength and relative phase of the $|0\rangle \leftrightarrow |e\rangle$ and $|1\rangle \leftrightarrow |e\rangle$ transitions. The Hamiltonian is turned on and off at $t = 0$ and $t = \tau$, respectively, controlled by $\Omega(t)$. The pulse envelopes are described as monochromatic. It is therefore assumed that $\Omega(t)$ is slowly varying on the time scales $\frac{1}{\nu_j}$, where ν_j is the frequency of the driving field addressing the $|j\rangle \leftrightarrow |e\rangle$ transition, so that the quasi-monochromatic approximation is valid. This is equivalent to the requirement that $\frac{\Delta \nu_j}{\nu_j} \ll 1$, where $\Delta \nu_j$ is the spectral width of the pulse [29]. For the rotating wave approximation to be valid, it is also necessary that $\Omega(t) \ll \nu_j$ [30]. Furthermore, we take $|0\rangle$ and $|1\rangle$ to define the one-qubit state space. The Λ configuration is illustrated in Fig. 1.

The pulse pairs are chosen such that ω_0 and ω_1 are time independent over the duration of each pulse pair. With this choice of parameters, the dark state $|d\rangle = -\omega_1|0\rangle + \omega_0|1\rangle$ decouples from the dynamics and the evolution is reduced to a simple Rabi oscillation between the bright state $|b\rangle = \omega_0^*|0\rangle + \omega_1^*|1\rangle$ and the excited state $|e\rangle$ [31]. The Rabi frequency is $\Omega(t)$ and the subspace $M(t)$ spanned by $|\psi_j(t)\rangle = e^{-i\int_0^t H^{(\text{na})}(t')dt'}|j\rangle = U(t,0)|j\rangle$, $j = 0,1$, undergoes a cyclic evolution if the pulse envelope satisfies $\int_0^\tau \Omega(t')\,dt' = \pi$. Under the above conditions, the final time evolution operator $U(\tau,0)$, projected onto the qubit space spanned by $\{|0\rangle,|1\rangle\}$, defines the traceless Hermitian holonomic one-qubit gate

$$U(C_{\mathbf{n}}) = \mathbf{n} \cdot \boldsymbol{\sigma}, \quad (2)$$

where $\mathbf{n} = (\sin\theta\cos\phi, \sin\theta\sin\phi, \cos\theta)$ is a unit vector, $C_{\mathbf{n}}$ is the evolution corresponding to $\omega_0/\omega_1 = -\tan(\theta/2)e^{i\phi}$, and $\boldsymbol{\sigma} = (\sigma_x, \sigma_y, \sigma_z)$ is a vector of the standard Pauli operators acting on $|0\rangle, |1\rangle$. Thus, any traceless Hermitian SU(2) operation can be implemented using a pulse pair. Two pairs of pulses corresponding to the unit vectors $\mathbf{n}$ and $\mathbf{m}$ applied sequentially results in

$$U(C) = U(C_{\mathbf{m}})U(C_{\mathbf{n}}) = \mathbf{m} \cdot \mathbf{n} + i\boldsymbol{\sigma} \cdot (\mathbf{m} \times \mathbf{n}), \quad (3)$$

which is an arbitrary SU(2) operation. Thus, $U(C)$ is a universal one-qubit gate. The evolution is purely geometric since $\langle\psi_j(t)|H^{(\text{na})}(t)|\psi_k(t)\rangle = \langle j|H^{(\text{na})}(t)|k\rangle = 0$, $j,k = 0,1$, for $t \in [0,\tau]$. C can be interpreted as the path of $M(t)$ in the space of all two-dimensional subspaces of the three-dimensional Hilbert space, i.e., the Grassmann manifold $G(3; 2)$.

B. The adiabatic gate

The adiabatic scheme proposed by Duan *et al.* [6] is implemented utilizing a tripod-type system, where three ground states $|0\rangle$, $|1\rangle$, and $|a\rangle$ are coupled to an excited state $|e\rangle$ by the driving fields. Thus, the adiabatic implementation requires coherent control over an additional level compared to the nonadiabatic implementation using a Λ system. The tripod configuration contains a two-dimensional dark subspace, dependent on the field couplings. The system is prepared in a dark state belonging to the computational subspace spanned by $|0\rangle$ and $|1\rangle$, and the field couplings are varied independently such that the system remains approximately in an instantaneous dark state in the limit of large run time T. More precisely, to remain in the adiabatic regime, the evolution in parameter space must be slow compared to the dynamical time scale of the system given by the energy difference between the dark and bright energy eigenstates. The Hamiltonian for this system in the rotating wave approximation is

$$\begin{aligned} H^{(\text{a})}(t) = \Omega[\omega_0(t/T)|e\rangle\langle 0| + \omega_1(t/T)|e\rangle\langle 1| \\ + \omega_a(t/T)|e\rangle\langle a| + \text{H.c.}], \quad (4) \end{aligned}$$

where we have assumed zero-detuned field couplings. For ideal gate implementation it is, however, necessary only that the field couplings are equally detuned. The tripod configuration is illustrated in Fig. 1. The field parameters are varied through a closed loop in parameter space. In this way, a universal set of one-qubit gates consisting of $U_1(\Gamma_1) = e^{i\frac{1}{2}\Gamma_1|1\rangle\langle 1|}$ and $U_2(\Gamma_2) = e^{i\Gamma_2\sigma_y}$, Γ_1 and Γ_2 being real numbers, can be realized.

The U_1 gate can be implemented by choosing $\omega_0 = 0$, $\omega_1 = -\sin(\vartheta/2)e^{i\varphi}$, and $\omega_a = \cos(\vartheta/2)$ and taking ϑ and φ around a loop c_1 in parameter space enclosing the solid angle $\Gamma_1 =$

$\int_{c_1} \sin\vartheta \, d\vartheta \, d\varphi$. The U_2 gate can be implemented by choosing $\omega_0 = \sin\vartheta \cos\varphi$, $\omega_1 = \sin\vartheta \sin\varphi$, and $\omega_a = \cos\vartheta$ and taking ϑ and φ around a loop c_2 in parameter space enclosing the solid angle $\Gamma_2 = \int_{c_2} \sin\vartheta \, d\vartheta \, d\varphi$.

III. ANALYSIS OF GATE ROBUSTNESS

There are two qualitatively different sources of error for the holonomic gates. One is open system effects caused by the interaction with the environment. The other is imperfect control of the parameters of the Hamiltonian due to unavoidable instabilities of the setup. These parameters are associated with the external driving fields used to control the system and are described as classical fields.

Among open system effects, decay of the excited state and dephasing are important. These will be considered in Sec. III B. The nonadiabatic scheme populates the excited state during the action of each pulse pair, and it is therefore crucial to study the resilience to decay as a function of the operation parameters. In the adiabatic implementation, the excited state is populated only infinitesimally, and therefore the adiabatic gates are robust against decay in the adiabatic limit. While decay is typically the dominant open system effect in trapped atomic systems [32], dephasing plays a central role in superconducting circuits [33,34].

Important sources of errors due to parametric instability are detuning and imperfect control of the parameters of the driving field. These will be considered in Sec. III C. Errors in detuning and pulse area in the nonadiabatic Abelian case for a two-level system have been analyzed in Ref. [35].

The gate performance under open-system effects and parameter errors is quantified in terms of the gate fidelity $\langle \chi | U^\dagger(C) \varrho_{\text{out}} U(C) | \chi \rangle$, where $U(C)$ is the desired gate operation and ϱ_{out} is the output state computed from the dynamics for the nonadiabatic and adiabatic gates with error sources. For the open system effects and detuning, the gate fidelities are computed numerically for 4000 input states $|\chi\rangle$, uniformly distributed over the Bloch sphere with respect to the Haar measure. The evolution of each input state is numerically integrated from the dynamical equations using the adaptive time step fourth order Runge-Kutta-Fehlberg (RKF45) method. In the numerical simulations the robustness to error sources is investigated using two test gates, the $\frac{\pi}{2}$ phase-shift gate $|j\rangle \mapsto e^{ij\pi/2}|j\rangle$, $j = 0,1$, and the Hadamard gate $|j\rangle \mapsto \frac{1}{\sqrt{2}}[(-1)^j|j\rangle + |j \oplus 1\rangle]$, $j = 0,1$. Nonadiabatic and adiabatic implementations of these gates are described in Sec. III A.

A. Test gates

1. Nonadiabatic test gates

In the nonadiabatic scheme, the $\frac{\pi}{2}$ phase-shift gate can be implemented by two pulse pairs, with the choice $\mathbf{n} = (\cos\phi, \sin\phi, 0)$ and $\mathbf{m} = (\cos\phi', \sin\phi', 0)$. The Hadamard gate can be implemented by a single-pulse pair with $\mathbf{n} = \frac{1}{\sqrt{2}}(1,0,1)$.

The π pulses used in the numerical simulation are hyperbolic secant pulses with maximal amplitude β. Explicitly, for the $\frac{\pi}{2}$ phase-shift gate we choose the two pulse pairs as $\Omega(t)(\omega_0, \omega_1) = \beta\text{sech}(\beta t)(-1,1)/\sqrt{2}$ and $\Omega(t - t_s)(\omega_0', \omega_1') =$
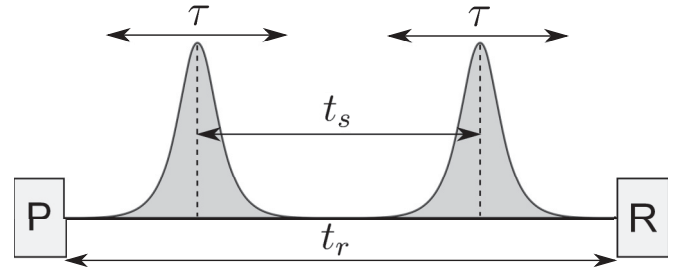

FIG. 2. Schematic illustration of the implementation of a nonadiabatic holonomic gate. The time t_r between preparation (P) and readout (R) of the qubit, the separation t_s of the pulse pairs, and the pulse length τ are indicated.

$\beta\text{sech}[\beta(t - t_s)](-1, e^{-i\pi/4})/\sqrt{2}$, where t_s is their temporal separation. For a given β, the temporal separation t_s must be chosen large enough so that the pulse overlap is negligible. This is a necessary condition to avoid any spurious dynamical contributions to the gate. The Hadamard gate is realized by a single pulse pair with shape $\Omega(t)(\omega_0, \omega_1) = \beta\text{sech}(\beta t)(1, (\sqrt{2} - 1))/\sqrt{2(2 - \sqrt{2})}$.

The pulses are truncated where the amplitude is $\beta/1000$, which gives the pulses a length $\tau = 2\frac{1}{\beta}\text{arcsech}(\frac{1}{1000})$. Therefore, the pulse duration in the nonadiabatic setting decreases with increasing β as a result of the pulse area being set to the fixed value π. This means that the total time t_r between preparation and readout can be decreased as well. Thus, by increasing β we effectively speed up the gate. The implementation of two pulse pairs and the relevant operation times τ, t_s, and t_r are illustrated in Fig. 2. Note that $\tau < t_s$ in order to avoid overlap of the pulses.

2. Adiabatic test gates

Next, we consider the adiabatic scheme. The $\frac{\pi}{2}$ phase-shift gate can be implemented by one loop in parameter space, while the Hadamard gate requires two loops. The ideal adiabatic $\frac{\pi}{2}$ phase-shift gate is generated in the $\Omega T \to \infty$ limit by varying the field couplings $\omega_0 = 0$, $\omega_1 = -\sin(\vartheta/2)e^{i\varphi}$, and $\omega_a = \cos(\vartheta/2)$ along the loop $(\vartheta, \varphi) = (0,0) \to (\frac{\pi}{2}, 0) \to (\frac{\pi}{2}, \pi) \to (0, \pi) \to (0, 0)$ at constant speed. Here $|0\rangle$ is decoupled from the excited state.

The ideal Hadamard gate is generated in the $\Omega T \to \infty$ limit by combining two loops. In the first loop, the field couplings are $\omega_0 = \sin\vartheta \cos\varphi$, $\omega_1 = \sin\vartheta \sin\varphi$, and $\omega_a = \cos\vartheta$, and these are varied along the loop $(\vartheta, \varphi) = (0,0) \to (\frac{\pi}{2}, 0) \to (\frac{\pi}{2}, -\frac{\pi}{4}) \to (0, -\frac{\pi}{4}) \to (0, 0)$ at constant speed. In the second loop, the field couplings are $\omega_0 = 0$, $\omega_1 = -\sin(\vartheta/2)e^{i\varphi}$, and $\omega_a = \cos(\vartheta/2)$, and these are varied along the loop $(\vartheta, \varphi) = (0,0) \to (\frac{\pi}{2}, 0) \to (\frac{\pi}{2}, 2\pi) \to (0, 2\pi) \to (0, 0)$. The curves in parameter space used to implement the adiabatic gates are illustrated in Fig. 3.

Since the run time T and the strength of the field coupling Ω are always finite for adiabatic gates, there will be nonadiabatic corrections that reduce the fidelity. These corrections are due to failure of the state to remain in the dark subspace during evolution. In Fig. 4 we show the fidelity for the adiabatic test gates for finite Ω and T. The fidelities are plotted as functions of the dimensionless quantity ΩT.

$(\vartheta, \varphi) = (0,0) \rightarrow (\frac{\pi}{2}, 0) \rightarrow (\frac{\pi}{2}, \pi) \rightarrow (0, \pi) \rightarrow (0,0)$

$(\vartheta, \varphi) = (0,0) \rightarrow (\frac{\pi}{2}, 0) \rightarrow$ $(\vartheta, \varphi) = (0,0) \rightarrow (\frac{\pi}{2}, 0) \rightarrow$

$(\frac{\pi}{2}, -\frac{\pi}{4}) \rightarrow (0, -\frac{\pi}{4}) \rightarrow (0,0)$ $(\frac{\pi}{2}, 2\pi) \rightarrow (0, 2\pi) \rightarrow (0,0)$
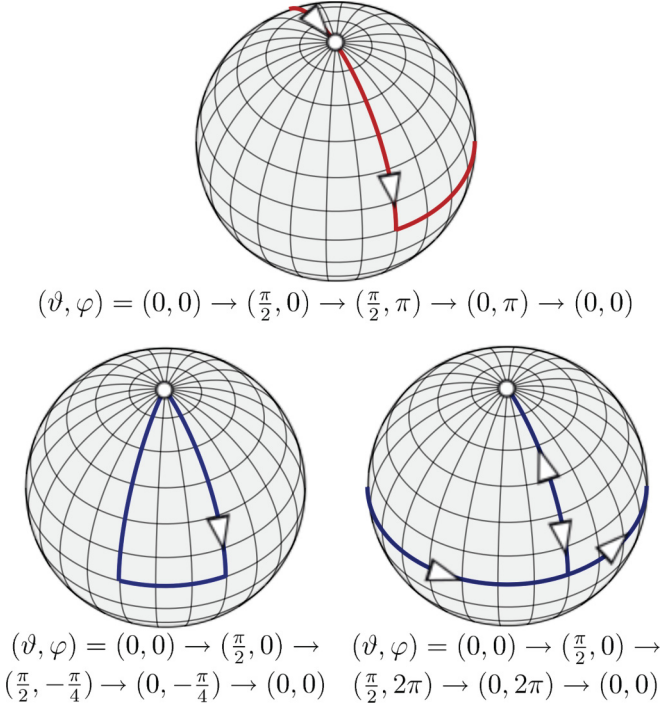
FIG. 3. (Color online) The curve in parameter space used to implement the adiabatic holonomic $\frac{\pi}{2}$ phase-shift gate (top) and the two curves in parameter space used to implement the Hadamard gate (bottom). The top and right bottom curves correspond to the field couplings $\omega_0 = 0$, $\omega_1 = -\sin(\vartheta/2)e^{i\varphi}$ and $\omega_a = \cos(\vartheta/2)$, while the left bottom curve corresponds to $\omega_0 = \sin\vartheta\cos\varphi$, $\omega_1 = \sin\vartheta\sin\varphi$ and $\omega_a = \cos\vartheta$.

The oscillatory behavior of the fidelities, as a function of ΩT, is due to nonadiabatic effects. These effects can be understood as a combination of modified holonomies, caused by changes in the path of the computational subspace, and nonzero dynamical phases. The revivals seen in the fidelities have been pointed out previously in Ref. [25]. Some of the revivals reach unit fidelity and these can therefore be used to implement the desired gates for finite ΩT. However in the nonadiabatic regime the gate is not holonomic since there are both dynamical and geometrical contributions to the gate operation. For the $\frac{\pi}{2}$ phase-shift gate the maximal fidelity (red line) is unity for all ΩT since $|0\rangle$ is decoupled from the dynamics.

B. Open system effects

1. Decay

To investigate the sensitivity of the nonadiabatic scheme to decay we assume that the time scale of the applied pulses is large compared to the time scale of the dynamics underlying the decay process, so that the Markovian approximation is valid. Given this, we further assume that the excited state decays to an auxiliary ground state level $|g\rangle$ [36] with a time-independent rate γ. We compare the sensitivity of the nonadiabatic implementations of the test gates with that of the corresponding adiabatic implementations of the gates. The decay is modeled by the Lindblad equation

$$\dot{\varrho}_t = -i[H(t),\varrho_t] + 2L\varrho_t L^\dagger - L^\dagger L\varrho_t - \varrho_t L^\dagger L, \quad (5)$$

where ϱ_t is the density operator, $L = \sqrt{\gamma}|g\rangle\langle e|$, and $H(t)$ is either $H^{(na)}(t)$ or $H^{(a)}(t)$.

In the nonadiabatic case, the constraint of having π pulses implies that the only experimentally controllable parameters of principal importance are the maximal coupling strength β and the total time between preparation and readout t_r. The dynamics of the gate can be described in terms of two dimensionless parameters. These can be chosen as β/γ and γt_r. When the pulse is a perfect π pulse the excited state is negligibly populated after the end of the pulse. Therefore, the relevant time scale for decay is the width of the pulse τ, which is proportional to $\frac{1}{\beta}$. Since $\gamma\tau \propto \frac{\gamma}{\beta}$ there is only one dynamically relevant dimensionless parameter.

The relevant operation parameters in the adiabatic case are the coupling strength Ω and run time T. The dynamics can be characterized by two dimensionless parameters, which can be chosen as ΩT and γT. In the simulations we consider both a fixed coupling strength Ω_0 and vary T and a fixed run time T_0 and vary Ω.

In Fig. 5 we show the fidelities of the test gates, computed from Eq. (5). The fidelities are plotted as functions of the dimensionless quantity β/γ in the nonadiabatic case, as well as $\Omega_0 T$ and ΩT_0 in the adiabatic case for fix coupling strength and fixed run time, respectively. For the adiabatic case, we have chosen $\Omega_0/\gamma = 12.5$, in the case of fixed coupling strength, and in the case of fixed run time we have chosen $\gamma T_0 = 8$ for the $\frac{\pi}{2}$ phase-shift gate and $\gamma T_0 = 32$ for the Hadamard gate. These choices are made to make the effect of decay non-negligible. Furthermore, in the nonadiabatic case we have
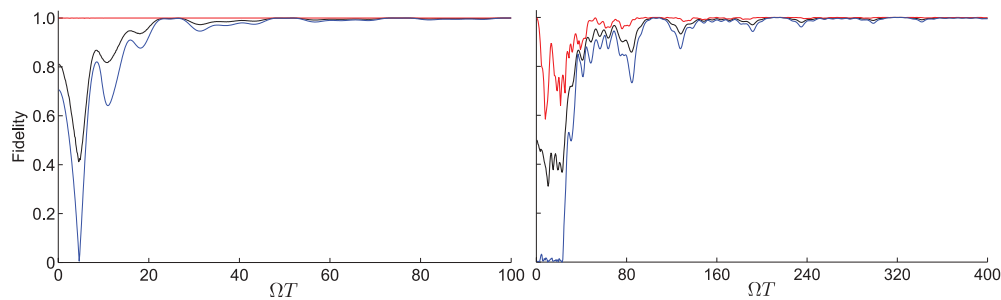

FIG. 4. (Color online) Influence of nonadiabatic corrections on the adiabatic holonomic $\frac{\pi}{2}$ phase-shift gate (left) and Hadamard gate (right). The effect is quantified from top to bottom in terms of maximum (red), average (black), and minimum (blue) fidelities. We plot the fidelities as functions of the dimensionless quantity ΩT, where Ω is the time-independent global strength of field couplings and T is the run time of the gate.
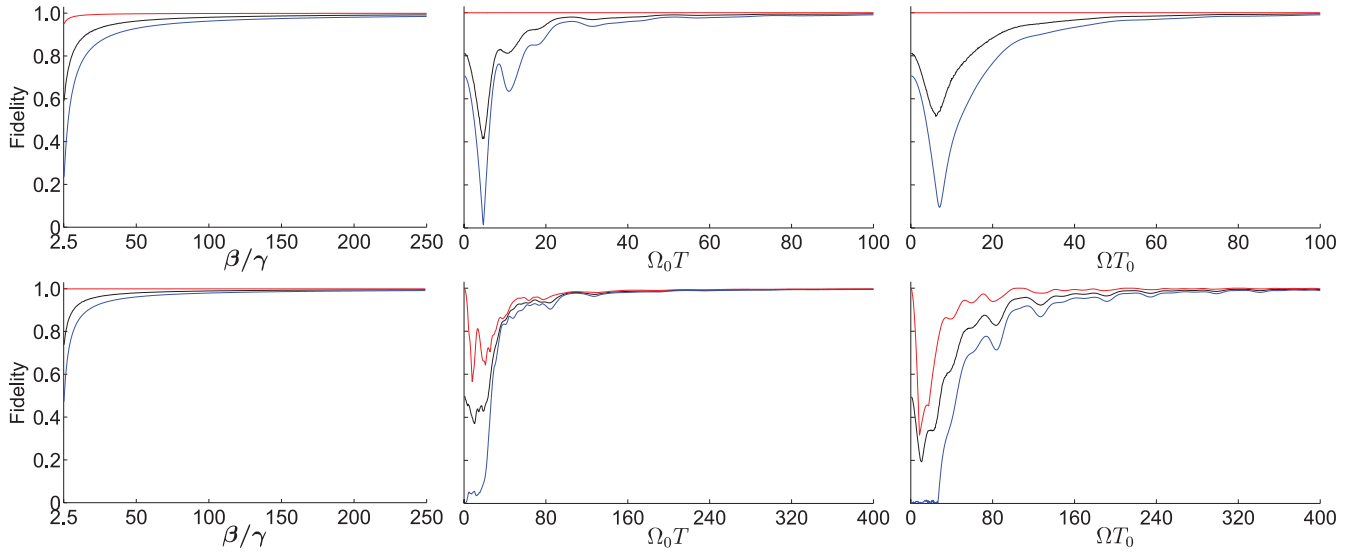
FIG. 5. (Color online) Influence of decay with rate γ of the excited state $|e\rangle$ on the nonadiabatic and adiabatic holonomic $\frac{\pi}{2}$ phase-shift gate (upper) and Hadamard gate (lower). The effect is quantified from top to bottom in terms of maximum (red), average (black), and minimum (blue) fidelities. The three panels show from left to right, the nonadiabatic gate with decay (left) and the adiabatic gate with decay, for a fixed coupling strength (middle) and fixed run time (right). Choosing hyperbolic secant π pulses with amplitude β, the nonadiabatic fidelities are plotted as functions of the dimensionless quantity β/γ. We plot the adiabatic fidelities as functions of the dimensionless quantities $\Omega_0 T$ and ΩT_0, where Ω is the time independent global strength of field couplings, T is the run time of the gate, and Ω_0 and T_0 are particular fixed values of these quantities. For the adiabatic gates we have chosen $\Omega_0/\gamma = 12.5$ for the case with fixed coupling strength and for the case of fixed run time we have chosen $\gamma T_0 = 8$ for the $\frac{\pi}{2}$ phase-shift gate and $\gamma T_0 = 32$ for the Hadamard gate. In the nonadiabatic case, we have chosen $\gamma t_s = 8$, where t_s is the temporal separation of the two pulses. t_s is chosen sufficiently large to avoid pulse overlap for the β/γ range shown in the left panels.

chosen $\gamma t_s = 8$, which guarantees that there is no pulse overlap for the β/γ range shown.

The fidelities of the nonadiabatic gates tend monotonically to unity in the large β/γ limit for both test gates (left panels). This demonstrates that the nonadiabatic holonomic test gates can be made robust to decay of the excited state by employing pulses that are sufficiently short compared to the decay time $\frac{1}{\gamma}$. For the Hadamard gate the maximal fidelity (red line) is identity for all β/γ. This is because it is implemented by a single pulse, and the dark state of the Hamiltonian corresponding to this pulse is left unchanged by the dynamics and hence unaffected by the decay. For the $\frac{\pi}{2}$ phase-shift gate no state is left unchanged by the gate operation, which explains why maximal fidelity is slightly decreased for small β/γ.

The stability of the adiabatic gates to decay of the excited state in the adiabatic limit is confirmed as the fidelities of the adiabatic gates tend to unity in the large ΩT limit. However, the fidelity of the revivals will no longer reach unity when there is decay of the excited state. In the adiabatic implementation of the $\frac{\pi}{2}$ phase-shift gate the maximal fidelity (red line) is identity since $|0\rangle$ is decoupled from the dynamics and therefore unaffected by the decay. For the Hadamard gate no state is decoupled from the dynamics, and therefore the maximum fidelity is low for small ΩT.

2. Dephasing

Dephasing is hard to eliminate in some implementations of holonomic gates, for example, in superconducting Josephson junctions [34]. Therefore, we study the robustness of the

nonadiabatic and adiabatic schemes to dephasing. More precisely, we consider dephasing in the $|0\rangle, |e\rangle$ and $|1\rangle, |e\rangle$ bases. The effect of dephasing is modeled by the Lindblad equation

$$\dot{\varrho}_t = -i[H(t), \varrho_t] + \sum_{i=0,1} (2L_{ke}\varrho_t L_{ke}^\dagger - L_{ie}^\dagger L_{ie}\varrho_t - \varrho_t L_{ie}^\dagger L_{ie}),$$

(6)

where ϱ_t is the density operator, $L_{ke} = \sqrt{\epsilon}(|e\rangle\langle e| - |k\rangle\langle k|)$ are the Lindblad operators, and $H(t)$ is either $H^{(na)}(t)$ or $H^{(a)}(t)$. We use the assumption that the time scale of the process underlying the dephasing is short compared to the time scale of the pulses (Markovian approximation). We again compare the resulting fidelities of the nonadiabatic implementations of the two test gates with those of their corresponding adiabatic implementations.

In the nonadiabatic case, the operation parameters are β and the total time t_r between preparation and readout. The two dimensionless parameters describing the dynamics are $\frac{\beta}{\epsilon}$ and ϵt_r. Since the qubit space is not a decoherence free subspace of the dephasing, the full time between preparation and readout is relevant for the fidelity of the gate operation. The best fidelity is thus achieved when the total time is reduced to only the time required to implement the gates. To study the effect of dephasing on gate operation we have therefore assumed that gates are implemented immediately following preparation and that readout is made immediately afterwards. This assumption reduces the relevant time to $\tau \propto \frac{1}{\beta}$, and the only relevant dimensionless parameter is therefore $\frac{\beta}{\epsilon}$.

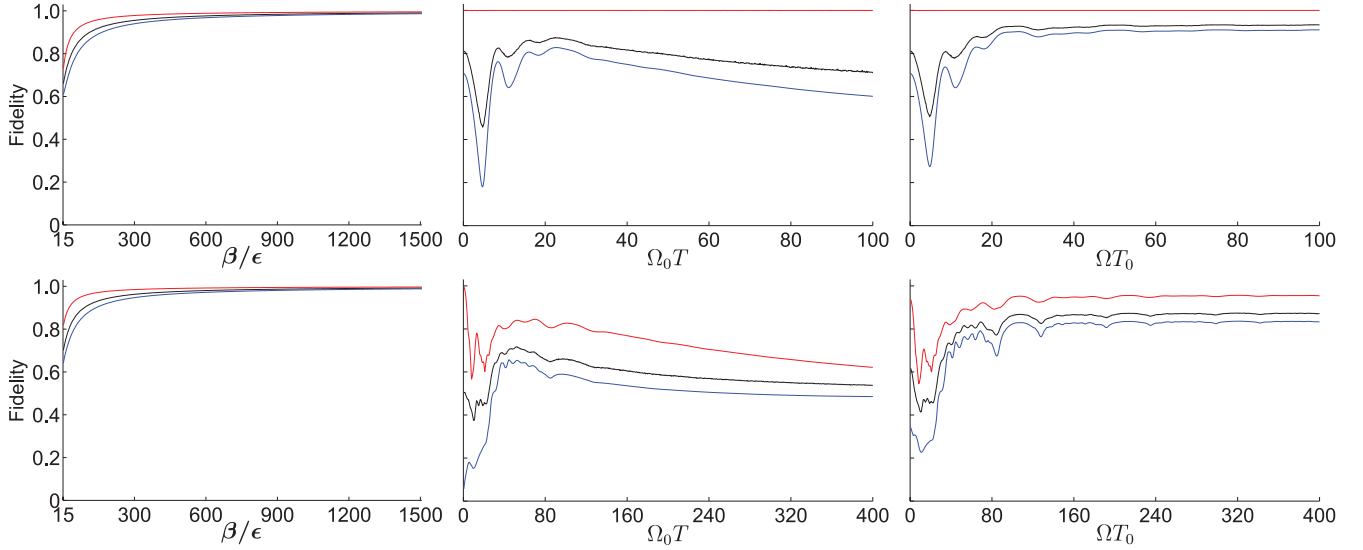FIG. 6. (Color online) Influence of dephasing in the $|0\rangle,|e\rangle$ and $|1\rangle,|e\rangle$ bases, on the nonadiabatic and adiabatic holonomic $\frac{\pi}{2}$ phase-shift gate (upper) and Hadamard gate (lower). The effect is quantified from top to bottom in terms of maximum (red), average (black), and minimum (blue) fidelities. The three panels show from left to right, the nonadiabatic gate with dephasing (left) and the adiabatic gate with dephasing, for a fixed coupling strength (middle) and fixed run time (right). Choosing hyperbolic secant π-pulses with amplitude β, the nonadiabatic fidelities are plotted as functions of the dimensionless quantity β/ϵ. We plot the adiabatic fidelities as functions of the dimensionless quantities $\Omega_0 T$ and ΩT_0, where Ω is the time-independent global strength of field couplings, T is the run time of the gate, and Ω_0 and T_0 are particular fixed values of these quantities. For the adiabatic gates, we have chosen $\Omega_0/\epsilon = 78.125$ for the case with fixed coupling strength, and for the case of fixed run time we have chosen $\epsilon T_0 = 0.16$ for the $\frac{\pi}{2}$ phase-shift gate and $\epsilon T_0 = 0.32$ for the Hadamard gate. In the nonadiabatic case, we have chosen $\epsilon t_s = 0.128$, where t_s is the temporal separation of the two pulses. t_s is chosen sufficiently large to avoid pulse overlap for the β/ϵ range shown in the left panels.

The relevant operation parameters in the adiabatic case are the coupling strength Ω and run time T, and the dimensionless parameters describing the dynamics can be chosen as ΩT and ϵT. In the simulations we consider both a fixed coupling strength Ω_0 and vary the run time, and a fixed run time T_0 and vary the coupling strength.

In Fig. 6 we show the fidelities of the test gates, computed using Eq. (6). The fidelities are plotted as functions of the dimensionless quantity β/ϵ in the nonadiabatic case, as well as $\Omega_0 T$ and ΩT_0 in the adiabatic case for fix coupling strength and fixed run time, respectively. For the adiabatic case we have chosen $\Omega_0/\epsilon = 78.125$, in the case of fixed coupling strength, and in the case of fixed run time we have chosen $\epsilon T_0 = 0.16$ for the $\frac{\pi}{2}$ phase-shift gate and $\epsilon T_0 = 0.32$ for the Hadamard gate. These choices are made to make the effect of dephasing non-negligible. Furthermore, in the nonadiabatic case we have chosen $\epsilon t_s = 0.128$, which guarantees that there is no pulse overlap for the β/ϵ range shown.

The fidelities of the nonadiabatic gates tend monotonically to unity in the large β/ϵ limit for both test gates (left panels). Thus, the nonadiabatic version of the holonomic $\frac{\pi}{2}$ phase-shift gate can be made resilient to the dephasing channel by employing sufficiently short pulses and reducing idle time before and after the pulses.

The adiabatic gates are not stable to dephasing in the limit $T \to \infty$, and we see a gradual decline in the fidelities as run time increases. If the run time is fixed and Ω is increased, the fidelities stabilize at some value below unity that is a function of the parameter ϵT_0. To have high fidelity in the adiabatic case it is necessary that Ω can be made large compared to ϵ so that

the adiabatic approximation is valid for a run time at which the effect of dephasing is still negligible. Alternatively, Ω should be large enough so that the effect of dephasing is negligible at some T corresponding to a revival of the fidelity.

C. Parametric control

1. Detuning

We assume that the $|j\rangle \leftrightarrow |e\rangle$ transition is driven by a laser pulse with frequency ν_j. The associated detuning is $\Delta_j = 2\pi \nu_j - \omega_{je}$, where ω_{je} is the corresponding energy spacing. Ideally, the detunings must vanish in the nonadiabatic case, while they must be all equal in the adiabatic setting. Here we examine the effect of deviations from these ideal values on the gate fidelity. To simplify the analysis, we limit the study to time independent detunings.

Nonzero detunings give rise to additional diagonal terms in the Hamiltonian. In the nonadiabatic case, we have

$$H_\Delta^{(na)}(t) = \Delta_0 |0\rangle\langle 0| + \Delta_1 |1\rangle\langle 1| + H^{(na)}(t), \qquad (7)$$

where $H^{(na)}(t)$ is the ideal Hamiltonian in Eq. (1). Similarly, in the adiabatic case, we have

$$H_\Delta^{(a)}(t) = \Delta_0 |0\rangle\langle 0| + \Delta_1 |1\rangle\langle 1| + \Delta_a |a\rangle\langle a| + H^{(a)}(t), \qquad (8)$$

where now $H^{(a)}(t)$ is the ideal Hamiltonian in Eq. (4). If two detunings are equal but different from the third, there will only be one dark state, and if all three detunings are different from each other, there will be no dark state at all. Thus, deviations from the $\Delta_0 = \Delta_1 = \Delta_a$ constraint destroy the dark state structure and the associated holonomy.
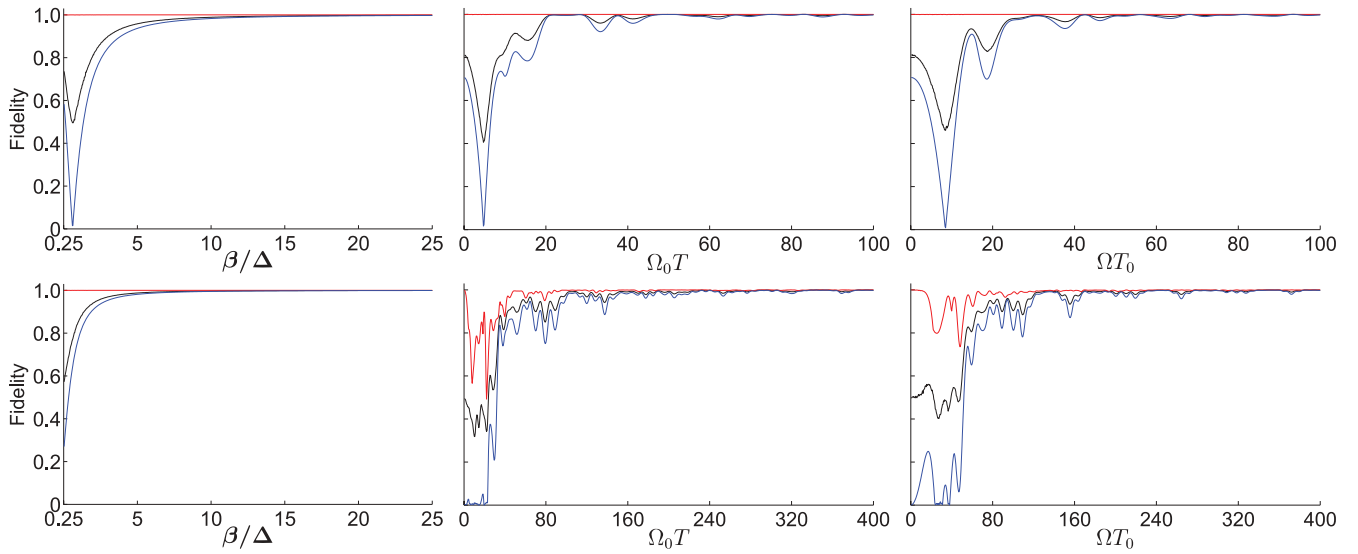
FIG. 7. (Color online) Influence of a constant mean detuning Δ and zero relative detuning on the nonadiabatic and adiabatic holonomic $\frac{\pi}{2}$ phase-shift gate (upper) and Hadamard gate (lower). The effect is quantified from top to bottom in terms of maximum (red), average (black), and minimum (blue) fidelities. The three panels show from left to right, the nonadiabatic gate with mean detuning (left) and the adiabatic gate with mean detuning, for a fixed coupling strength (middle) and fixed run time (right). Choosing hyperbolic secant π pulses with amplitude β, the nonadiabatic fidelities are plotted as functions of the dimensionless quantity β/Δ. We plot the adiabatic fidelities as functions of the dimensionless quantities $\Omega_0 T$ and ΩT_0, where Ω is the time-independent global strength of field couplings, T is the run time of the gate, and Ω_0 and T_0 are particular fixed values of these quantities. For the adiabatic gates we have chosen $\Omega_0/\Delta_{01a} = 6.25$ for the case with fixed coupling strength, and for the case of fixed run time we have chosen $\Delta_{01a} T_0 = 16$ for the $\frac{\pi}{2}$ phase-shift gate and $\Delta_{01a} T_0 = 64$ for the Hadamard gate. In the nonadiabatic case we have chosen $\Delta t_s = 80$, where t_s is the temporal separation of the two pulses. t_s is chosen sufficiently large to avoid pulse overlap for the β/Δ range shown in the left panels.

Note that we express $H_\Delta^{(na)}(t)$ and $H_\Delta^{(a)}(t)$ in frames that are "co-rotating" with their respective detuned driving fields. Therefore, to compare the output of the gate operation $\varrho_{out}(t)$ generated by the detuned Hamiltonians, with the output of the desired gate operation $U(C)$, we must transform $\varrho_{out}(t)$ to the frame co-rotating with the ideal driving fields. This is done through the transformation $\varrho_{out}(t) \rightarrow e^{iSt}\varrho_{out}(t)e^{-iSt}$, where $S = \Delta_0|0\rangle\langle 0| + \Delta_1|1\rangle\langle 1|$ in the nonadiabatic case and $S = \Delta_0|0\rangle\langle 0| + \Delta_1|1\rangle\langle 1| + \Delta_a|a\rangle\langle a|$ in the adiabatic case. Note also that these frame rotations will remove the effect of the diagonal terms in Eqs. (7) and (8) for the part of the evolution where the driving fields vanish.

We study two principal cases. First, all detunings are set equal, and second, some of the detunings are assumed to be different. These cases are naturally captured by the mean and relative detunings. In the nonadiabatic setting, these read $\Delta = \frac{\Delta_0+\Delta_1}{2}$ and $\delta = \frac{\Delta_0-\Delta_1}{2}$, respectively. In the adiabatic case, we have the mean detuning $\Delta_{01a} = \frac{\Delta_0+\Delta_1+\Delta_a}{3}$ and two independent relative detunings $\delta_{01} = \frac{\Delta_0-\Delta_1}{2}$ and $\delta_{0a} = \frac{\Delta_0-\Delta_a}{2}$. In some implementations it may be easier to control the relative detuning of the driving fields than the mean detuning.

First, we investigate how gate operation is affected in the nonadiabatic case when a constant mean detuning is introduced and the relative detuning is zero. For comparison we also include the adiabatic implementations with the same mean detuning and all relative detunings zero.

The dynamics of the nonadiabatic gate with $\Delta \neq 0$ and $\delta = 0$ depends on two dimensionless parameters that can be chosen as β/Δ and Δt_r. However, since the entire dynamics

is generated by the driving fields, the relevant time is the pulse length $\tau \propto \frac{1}{\beta}$. Thus, β/Δ is the only relevant dimensionless parameter.

The relevant operation parameters in the adiabatic case are the coupling strength Ω and run time T, and the dimensionless parameters describing the dynamics are ΩT and ΔT. In the simulations we consider both a fixed coupling strength Ω_0 and vary the run time and a fixed run time T_0 and vary the coupling strength.

In Fig. 7 we show the fidelities of the gates computed using Eqs. (7) and (8) in the nonadiabatic and adiabatic case, respectively. The fidelities are plotted as functions of the dimensionless quantity β/Δ in the nonadiabatic case, as well as $\Omega_0 T$ and ΩT_0 in the adiabatic case for fix coupling strength and fixed run time, respectively. We choose $\Omega_0/\Delta_{01a} = 6.25$ in the case of fixed coupling strength. In the case of fixed run time, we take $\Delta_{01a} T_0 = 16$ for the $\frac{\pi}{2}$ phase-shift gate and $\Delta_{01a} T_0 = 64$ for the Hadamard gate. Furthermore $\Delta t_s = 80$, which guarantees that there is no pulse overlap for the β/Δ range shown in the figure.

With a constant mean detuning and zero relative detuning, the fidelities of the nonadiabatic gates tend to unity in the large β/Δ limit (left panels). This demonstrates that the nonadiabatic versions of the holonomic test gates can be made robust to constant mean detuning by employing sufficiently short pulses. The adiabatic scheme is stable to constant mean detuning in the $\Omega T \rightarrow \infty$ limit.

Next, we consider nonzero relative detuning. The adiabatic implementation of the $\frac{\pi}{2}$ phase-shift gate does not involve any driving field coupled to the $|0\rangle \leftrightarrow |e\rangle$ transition. For this reason
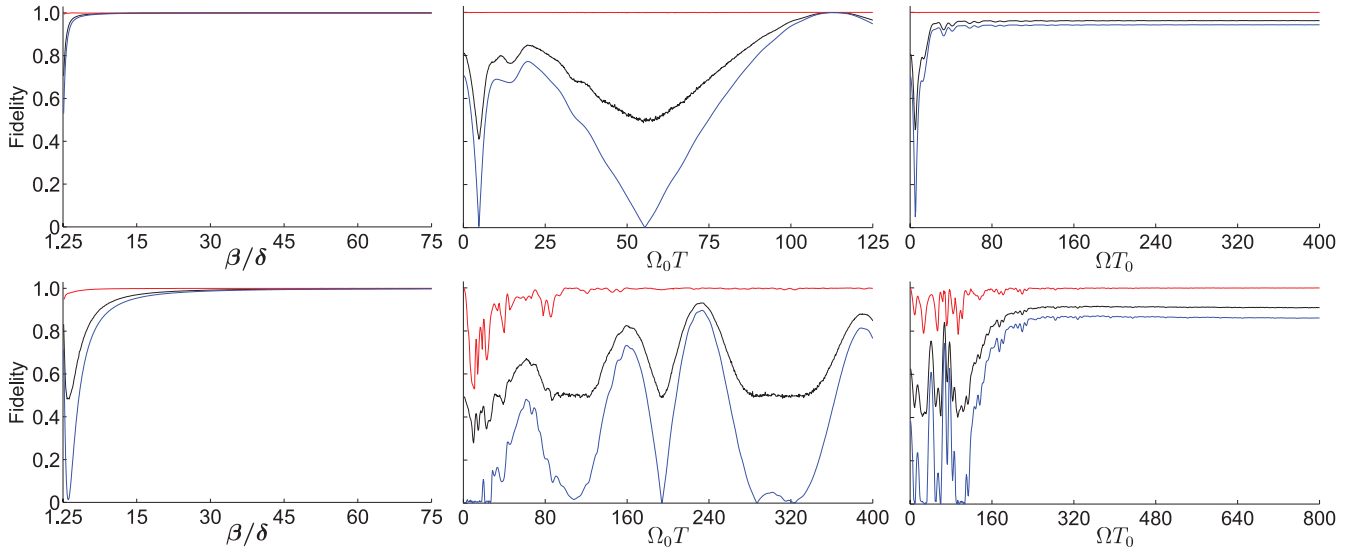
FIG. 8. (Color online) Influence of a constant relative detuning δ on the nonadiabatic and adiabatic holonomic $\frac{\pi}{2}$ phase-shift gate (upper) and Hadamard gate (lower). The effect is quantified from top to bottom in terms of maximum (red), average (black), and minimum (blue) fidelities. The three panels show, from left to right, the nonadiabatic gate with relative detuning and the adiabatic gate with relative detuning, for a fixed coupling strength (middle) and fixed run time (right). Choosing hyperbolic secant π pulses with amplitude β, the nonadiabatic fidelities are plotted as functions of the dimensionless quantity β/δ. We plot the adiabatic fidelities as functions of the dimensionless quantities $\Omega_0 T$ and ΩT_0, where Ω is the time-independent global strength of field couplings, T is the run time of the gate, and Ω_0 and T_0 are particular fixed values of these quantities. For the adiabatic gates we have chosen $\Omega_0/\delta = 6.25$ for the case with fixed coupling strength, and for the case of fixed run time we have chosen $\delta T_0 = 2$ for the $\frac{\pi}{2}$ phase-shift gate and $\delta T_0 = 64$ for the Hadamard gate. In the nonadiabatic case we have chosen $\delta t_s = 16$, where t_s is the temporal separation of the two pulses. t_s is chosen sufficiently large to avoid pulse overlap for the β/δ range shown in the left panels.

we consider the case where the only nonzero detuning is $\delta \equiv \Delta_1$ of the driving field associated with the $|1\rangle \leftrightarrow |e\rangle$ transition.

The relevant dimensionless dynamical parameter for the nonadiabatic gates is β/δ. The relevant operation parameters in the adiabatic case are the coupling strength Ω and run time T, and the dimensionless parameters describing the dynamics are ΩT and δT. In the simulations we consider both a fixed coupling strength Ω_0 and vary T and a fixed run time T_0 and vary Ω.

In Fig. 8 we show the fidelities of the test gates computed using Eq. (7) and (8) in the nonadiabatic and adiabatic case, respectively. The fidelities are plotted as functions of the dimensionless quantity β/δ in the nonadiabatic case, as well as $\Omega_0 T$ and ΩT_0 in the adiabatic case for fix coupling strength and fixed run time, respectively. We have chosen $\Omega_0/\delta = 6.25$ in the case of fixed coupling strength, while in the case of fixed run time, we take $\delta T_0 = 2$ for the $\frac{\pi}{2}$ phase-shift gate and $\delta T_0 = 64$ for the Hadamard gate. Furthermore, $\delta t_s = 16$, which guarantees that there is no pulse overlap for the β/δ range shown in the figure.

With constant relative detuning, the fidelities of the nonadiabatic gates tend to unity in the large β/δ limit (left panels). The behavior is similar to the case with nonzero mean detuning. The adiabatic gates, on the other hand, are unstable to relative detuning and do not converge to any value of the fidelity when run time T is increased while the coupling strength is fixed. Instead, the mean fidelity as a function of T is an oscillating function. If the run time is fixed and Ω is increased the fidelities stabilize at some value that is a function of the parameter δT_0 and typically not unity.

The nonadiabatic gates can thus be made resilient to relative detuning by using short enough pulses. One way to have high fidelity in the adiabatic case, is to choose T corresponding to a maximum in the oscillating mean fidelity. This, however, requires precise knowledge of the relative detuning. Without such knowledge it must be possible to choose Ω/δ sufficiently large so that the first decline in fidelity due to relative detuning becomes significant only at run times larger than the T required for the adiabatic approximation to be valid.

2. Driving field parameters

Control of the pulse envelope and the relative amplitudes and phases of the two driving fields is of crucial importance to gate operation. To study the effect of errors in the driving fields, we make the assumption that the deviations from the ideal case are such that the relative strength and relative phase of the $|0\rangle \leftrightarrow |e\rangle$ and $|1\rangle \leftrightarrow |e\rangle$ transitions are time independent during the implementation of a pulse pair. Given this assumption the Hamiltonian can be written

$$\widetilde{H}(t) = \widetilde{\Omega}(t)(\widetilde{\omega}_0 |e\rangle\langle 0| + \widetilde{\omega}_1 |e\rangle\langle 1| + \text{H.c.}) \equiv \widetilde{\Omega}(t)\widetilde{H}_0, \quad (9)$$

where $\widetilde{\Omega}(t)$ is the nonideal pulse envelope and $\widetilde{\omega}_j$ are the nonideal relative strength and phase of the transitions satisfying $|\widetilde{\omega}_0|^2 + |\widetilde{\omega}_1|^2 = 1$. Since the implementation of the nonadiabatic gates depends only on the area of the two pulses in each pulse pair and not on the exact shape, gate operation is robust to area-preserving deviations in the shape. Only the deviation of $a \equiv \int_0^\tau \widetilde{\Omega}(t)\,dt$ from π is relevant.

If we introduce the notation $H \equiv \Omega(t)H_0$ for the ideal Hamiltonian we can express the error due to the deviations in terms of the fidelity as

$$\mathcal{F}(\psi) = |\langle\psi|e^{i\pi H_0}e^{-ia\widetilde{H}_0(t)}|\psi\rangle|^2, \quad (10)$$

where $|\psi\rangle$ is an arbitrary normalized input qubit state. Using that $H_0^{2n} = H_0^2$ and $H_0^{2n-1} = H_0$ for $n = 1, 2, \ldots$, we can see that $e^{i\pi H_0} = \hat{1} - 2H_0^2$. Similarly $\widetilde{H}_0^{2n} = \widetilde{H}_0^2$ and $\widetilde{H}_0^{2n+1} = \widetilde{H}_0$ implies that $e^{-ia\widetilde{H}_0} = \hat{1} - (1 - \cos a)\widetilde{H}_0^2 - i(\sin a)\widetilde{H}_0$. Using this and the fact that the expectation value with respect to $|\psi\rangle$ of any product of an odd number of H_0 and $\widetilde{H}_0$ vanishes, we can express the fidelity as

$$\mathcal{F}(\psi) = \left|\langle\psi|1 - 2H_0^2 - (1 - \cos a)\left(\widetilde{H}_0^2 - 2H_0^2\widetilde{H}_0^2\right)|\psi\rangle\right|^2. \quad (11)$$

Assuming that $a = \pi + \delta a$ and $\widetilde{H}_0 = H_0 + \delta H_0$, where δa and $\delta H_0 = \delta\omega_0|e\rangle\langle 0| + \delta\omega_1|e\rangle\langle 1| + \text{H.c.}$ are small, we can expand the fidelity to second order in the deviations. This gives

$$\begin{aligned}\mathcal{F}(\psi) \approx{}& 1 - \delta a^2\langle\psi|H_0^2|\psi\rangle - 4\langle\psi|\delta H_0^2|\psi\rangle \\ &+ 4\langle\psi|H_0^2\delta H_0^2 + \delta H_0^2 H_0^2|\psi\rangle \\ &+ 4\langle\psi|[H_0, \delta H_0 + H_0\delta H_0 H_0]|\psi\rangle^2. \end{aligned} \quad (12)$$

Averaging over all input states gives the average fidelity

$$\mathcal{F}_{\text{av}} \approx 1 - \tfrac{1}{2}\delta a^2 - 2(|\delta\omega_0|^2 + |\delta\omega_1|^2) + 4|\delta\omega_0\omega_0^* + \delta\omega_1\omega_1^*|^2. \quad (13)$$

Thus, we can see that the one-qubit nonadiabatic holonomic gate is robust to first order in the deviations in the pulse area as well as in the relative phase and strength of the transitions. The error incurred by the incorrect parameters can be understood as a failure of the subspace $M(t)$ to follow the correct path. If the area of the pulses deviates from π the state will not return to the computational subspace, and the final state will have a nonzero amplitude in the excited state. If the pulse area is π, the state will return to the computational subspace, but the gate operation will not be the desired one unless $\frac{\widetilde{\omega}_0}{\omega_0} = \frac{\widetilde{\omega}_1}{\omega_1} = e^{i\alpha}$ for some $\alpha \in \mathbb{R}$ amounting to a $e^{i\alpha}$ phase shift of both ω_0 and ω_1.

A special case is when there is a deviation in the pulse area but correct relative strength and phase of the couplings. The second order dependence of the fidelity on δa in this case is consistent with the result of Ref. [35] for the Abelian case.

Although the above deviations in the parameters can lead to a gate operation that is not the desired one, the evolution is nevertheless still purely geometric during the implementation of the gate. This is in contrast to the error caused by detuning, where the reduced fidelity is due to the combined effect of modified holonomies and dynamical phases, and to the case with open system effects where the state evolves into a mixture of states that pick up different combinations of holonomies and dynamical phases. Another difference is that the error introduced by incorrect parameters is independent of the run time of the gate.

IV. CONCLUSIONS

The nonadiabatic gate can be made resilient to decay of the excited state and to constant mean and relative detunings by employing pulses that are sufficiently short compared to the time scales of the decay and detuning. If the idle time between preparation of the qubit and readout can be made negligible, the gate will also be resilient to dephasing in the $|e\rangle, |1\rangle$ and $|e\rangle, |0\rangle$ bases, in the limit of short pulses. It is therefore of critical importance for the implementation of such gates that the pulse height β can be made sufficiently large relative to the dynamical parameters describing these sources of error.

There is a principal upper limit on how fast the pulses can be implemented given by the breakdown of the quasi-monochromatic approximation when the pulse changes rapidly compared to the oscillations of the driving field. If the quasi-monochromatic approximation fails, there will be non-negligible frequency components of the driving field other than the desired one. These may couple to other transitions in the system and reduce fidelity of the gate. There is also a limit given by the breakdown of the rotating wave approximation when the ratio of the pulse height to either of the energy spacings ω_{je}, $j = 0$ or 1, becomes too large. This causes a non-negligible Bloch-Siegert shift [30,37] of the $|j\rangle \leftrightarrow |e\rangle$ transition resonance frequency due to the effect of the counter-rotating terms that can no longer be neglected. Furthermore, the analysis of the sensitivity to open-system effects is valid only when the Markovian approximation holds. Thus, if the pulse duration is decreased to a point where it becomes comparable to the time scale of the dynamical processes underlying the open system effects, the analysis using Lindblad's equation is no longer valid, and memory effects of the environment must be taken into account.

Control over the pulse shape is important only to the extent that the pulse area must be π. Moreover, the fidelity depends on small deviations in the pulse area and the other parameters of the driving fields only to second order. The gate cannot be made more robust to this source of error by decreasing run time.

In comparison, the adiabatic gates are robust to decay and mean detuning in the limit of large run time. They are, however, not robust to dephasing and relative detuning in this limit. Resilience to these sources of error in the adiabatic case requires that the field coupling strengths can be made large compared to the dephasing and relative detuning parameters, and that the run time can be chosen sufficiently small to make the error due to relative detuning or dephasing negligible. The requirements on the operation parameters for high fidelity gate implementation in the presence of dephasing or relative detuning are thus qualitatively similar to those for the nonadiabatic gate in the sense that the coupling strength must be increased and the run time decreased.

To fully address the issue of robustness of the nonadiabatic scheme for quantum computation one must also analyze the robustness of the two-qubit gate proposed in Ref. [9]. The two-qubit gate involves coupled Λ systems, which could be implemented using, for example, trapped ions coupled via collective spatial vibrations as in the Sørensen-Mølmer ion trap scheme [38]. In addition to errors emanating from imperfections in the driving fields and the interaction of the Λ systems with the environment, the analysis would have to involve errors originating from the coupling mechanism as well.

[1] P. Zanardi and M. Rasetti, Phys. Rev. Lett. **79**, 3306 (1997).

[2] E. Knill, R. Laflamme, and L. Viola, Phys. Rev. Lett. **84**, 2525 (2000).

[3] A. Y. Kitaev, Ann. Phys. (NY) **303**, 2 (2003).

[4] P. Zanardi and M. Rasetti, Phys. Lett. A **264**, 94 (1999).

[5] J. Pachos and P. Zanardi, Int. J. Mod. Phys. B **15**, 1257 (2001).

[6] L. M. Duan, J. I. Cirac, and P. Zoller, Science **292**, 1695 (2001).

[7] L. Faoro, J. Siewert, and R. Fazio, Phys. Rev. Lett. **90**, 028301 (2003).

[8] P. Solinas, P. Zanardi, N. Zanghì, and F. Rossi, Phys. Rev. B **67**, 121307 (2003).

[9] E. Sjöqvist, D. M. Tong, L. M. Andersson, B. Hessmo, M. Johansson, and K. Singh, New J. Phys. **14**, 103035 (2012).

[10] G. F. Xu, J. Zhang, D. M. Tong, E. Sjöqvist, and L. C. Kwek, Phys. Rev. Lett. **109**, 170501 (2012).

[11] V. Azimi Mousolou, C. M. Canali, and E. Sjöqvist, arXiv:1209.3645.

[12] A. Y. Kitaev, Russ. Math. Surv. **52**, 1191 (1997).

[13] D. Gottesman, arXiv:quant-ph/9705052.

[14] J. Preskill, Proc. R. Soc. Lond. Ser. A **454**, 385 (1998).

[15] A. M. Steane, Phys. Rev. A **68**, 042322 (2003).

[16] E. Knill, Nature (London) **434**, 39 (2005).

[17] V. I. Kuvshinov and A. V. Kuzmin, Phys. Lett. A **316**, 391 (2003).

[18] P. Solinas, P. Zanardi, and N. Zanghì, Phys. Rev. A **70**, 042316 (2004).

[19] P. V. Buividovich and V. I. Kuvshinov, Phys. Rev. A **73**, 022336 (2006).

[20] C. Lupo, P. Aniello, M. Napolitano, and G. Florio, Phys. Rev. A **76**, 012309 (2007).

[21] D. Ellinas and J. Pachos, Phys. Rev. A **64**, 022310 (2001).

[22] I. Fuentes-Guridi, F. Girelli, and E. Livine, Phys. Rev. Lett. **94**, 020503 (2005).

[23] A. Trullo, P. Facchi, R. Fazio, G. Florio, V. Giovanetti, and S. Pascazio, Laser Phys. **16**, 1478 (2006).

[24] D. Parodi, M. Sassetti, P. Solinas, P. Zanardi, and N. Zanghì, Phys. Rev. A **73**, 052304 (2006).

[25] G. Florio, P. Facchi, R. Fazio, V. Giovannetti, and S. Pascazio, Phys. Rev. A **73**, 022327 (2006).

[26] G. Florio, Open Syst. Inf. Dyn. **13**, 263 (2006).

[27] D. Parodi, M. Sassetti, P. Solinas, and N. Zanghì, Phys. Rev. A **76**, 012337 (2007).

[28] D. Møller, L. B. Madsen, and K. Mølmer, Phys. Rev. A **77**, 022306 (2008).

[29] L. Mandel and E. Wolf, *Optical Coherence and Quantum Optics* (Cambridge University Press, Cambridge, 1995), p. 160.

[30] F. Bloch and A. Siegert, Phys. Rev. **57**, 522 (1940).

[31] M. Fleischhauer and A. S. Manka, Phys. Rev. A **54**, 794 (1996).

[32] G. K. Brennen, C. M. Caves, P. S. Jessen, and I. H. Deutsch, Phys. Rev. Lett. **82**, 1060 (1999).

[33] I. Chiorescu, Y. Nakamura, C. J. P. M. Harmans, and J. E. Mooij, Science **299**, 1869 (2003).

[34] J. Koch, T. M. Yu, J. Gambetta, A. A. Houck, D. I. Schuster, J. Majer, A. Blais, M. H. Devoret, S. M. Girvin, and R. J. Schoelkopf, Phys. Rev. A **76**, 042319 (2007).

[35] J. T. Thomas, M. Lababidi, and M. Tian, Phys. Rev. A **84**, 042335 (2011).

[36] A numerical comparison of the different cases where $|e\rangle$ decays to either $|g\rangle$ or one of the levels $|0\rangle$ or $|1\rangle$ in the nonadiabatic case, and $|0\rangle$, $|1\rangle$ or $|a\rangle$ in the adiabatic case, shows that the differences in the fidelity of gate operation are small and has the same qualitative dependence on operation parameters.

[37] L. Allen and J. H. Eberly, *Optical Resonance and Two-Level Atoms* (Dover, New York, 1987), pp. 47–51

[38] A. Sørensen and K. Mølmer, Phys. Rev. Lett. **82**, 1971 (1999).